Earthquakes and Structures, *Vol. 12, No. 6 (2017) 591-601*
DOI: https://doi.org/10.12989/eas.2017.12.6.591

Seismic retrofitting of a tower with shear wall in UHPC based dune sand

Abderraouf Trabelsi[1,2a], Zied Kammoun[*3,4] and Aouicha Beddey[5b]

[1]Université de Tunis El Manar, Ecole Nationale d'Ingénieurs de Tunis, LR-03-ES05 Laboratoire de Génie Civil, 1002, Tunis, Tunisia
[2]Académie Militaire département génie civil fondouk jadid
[3]Université de Tunis El Manar, École nationale d'ingénieurs de Tunis, LR11ES16, Laboratoire de matériaux, optimisation et énergie pour la durabilité, B.P. 37, 1002, Tunis-Belvédère, Tunisia
[4]Université de Carthage, Institut Supérieur des Technologies de l'Environnement de l'Urbanisme et du Bâtiment, 2 Rue de l'Artisanat Charguia 2, 2035 Tunis
[5]Centre d'Etudes Techniques et d'Essais de Construction (C.E.T.E.C), Av, 15 Octobre 1009, Ouardia, Tunisia

(Received November 4, 2016, Revised May 27, 2017, Accepted May 28, 2017)

Abstract. To prevent or limit the damage caused by earthquakes on existing buildings, several retrofitting techniques are possible. In this work, an ultra high performance concrete based on sand dune has been formulated for use in the reinforcement of a multifunctional tower in the city of Skikda in Algeria. Tests on the formulated ultra high performance concrete are performed to determine its characteristics. A nonlinear dynamic analysis, based on the "Pushover" method was conducted. The analysis allowed an optimization of the width of reinforced concrete walls used in seismic strengthening. Two types of concrete are studied, the ordinary concrete and the ultra high performance concrete. Both alternatives are compared with the reinforcement with carbon fibers and by base isolation retrofit design.

Keywords: UHPC; dune sand; seismic; retrofitting; shear wall; pushover

1. Introduction

Earthquakes strike every year in different regions of the globe, causing human and material damage. North Africa, particularly Algeria, is likely to be subject to strong earthquakes (Fig. 1). Historically, among the most significant earthquakes we can cite the earthquake of Chlef of 1980 following which the Algerien seismic regulations (RPA) have been established.

We can also mention the earthquake of Boumerdes (2003), during which the structures built according to the current standards have suffered considerable damage, thesis showed the vulnerability of reinforced concrete (RC) framed structures, widely used in construction in Algeria. Since the Boumerdes earthquake, the Algerian seismic code was reviewed, and retrofitting become necessary for older buildings well as for recently completed buildings.

According to Mazza (2015), traditional methods for the seismic reinforcement can be classified into two categories: one is based on increasing strength and stiffness, by adding new structural elements to the system (e.g., Reinforced concrete RC shear wall) and the other is based on mass reduction to reduce the demand.

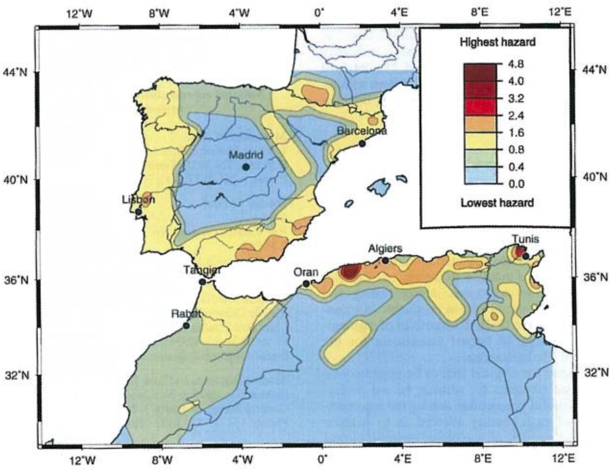

Fig. 1 Earthquake hazard map of the Ibero-Maghreb region. PGA (m/S^2) with 90% probability of non-exceedance in 50 years (Jiménez *et al.* 1999)

Modern methods for the seismic reinforcement, based on new techniques and materials, can be classified in three categories; modification of damage and collapse modes of the structure to eliminate possible sources of brittle failures, increasing deformability at the base of the building to reduce the transmission of the seismic loads to the superstructure, and adding damping to reduce the seismic demand capacity.

In Algeria, among all the available techniques, the RC shear walls are the most used as seismic solution. But the implementation requires is a major intervention on the

∗Corresponding author, Ph.D.
E-mail: kammounzied@yahoo.fr
[a]Ph.D.
E-mail: abederraouftrabelsi@gmail.com
[b]Professor
E-mail: beddey@cetec.nat.tn

http://www.techno-press.com/journals/eas&subpage=7
ISSN: 2092-7614 (Print), 2092-7622 (Online)

building and therefore, the reduction of the scale of this intervention is a priority which can only be achieved by improving the characteristics of the used concrete.

High Performance Concrete (HPC) is a high compressive strength concrete exceeding 50 MPa. The UHPC (Ultra High Performance Concrete) has on even high compressive strength which by definition exceeds 100 MPa.

The UHPC is usually used for building towers and bridges (Konkov 2013, D’aloia *et al.* 2003). But in North African countries, it is rarely used. This is due partly to the high cost of importing material used in the production as silica fume.

However, the desert dune sand is an abundant fine aggregate in these countries, and with its high composition in silica it can be a very inexpensive alternative to these sub-Saharan regions for the production of HPC and UHPC. Until now, several attempts to use the dune sand in formulations of concrete have been conducted in Tunisia, Algeria, Oman and Australia (Rmili *et al.* 2009, Bouziani 2013, Zeghichi *et al.* 2012, Al-Harthy *et al.* 2007, Luo *et al.* 2013). If for some researchers the objective was to formulate a self-compacting concrete, others have been able to obtain high strength concrete with a compressive strength close to 60 MPa.

In this work, a formulation of the UHPC based on dune sand is developed using the Dreux method. The mechanical properties of concrete are studied using tests. The elaborated UHPC is used for paraseismic reinforcement of a multifunctional tower located on the heights of the city of Skikda northeast of Algeria, 150 km from the Tunisian border.

In this paper, we analyse an existing tower in algeria before and after retrofitting by RC shear walls made with ordinary concrete, and with sand dune based UHPC. To investigate the technical and economical impact of the use of these systems, a comparative study was performed. A comparison was made between the RC shear walls retrofit and the retrofit with carbon fibers and insulators at the base.

In our study, we use the nonlinear static pushover analysis (which is a simplified pseudo-static analysis), based on the approximation of the displacement of the system with several degrees of freedom by the spectral response of a system with a single degree of freedom (Fajfar 1999, Chopra *et al.* 2002).

2. General description

Algeria, and specially his northern part , which lies near the borderline separating the African Plate from the Eurasian Plate, has a high seismic activity. This activity concerns the major part of the population, buildings and facilities.

Moreover, several studies show that the composition of the building stock in Algeria is constituted in its greater part of reinforced concrete constructions.

Whether it is in Tizi-Ouzou (Cherifi *et al.* 2015), Algiers (Ousalem 2005) or Constantine (Boukri *et al.* 2014), the neighbouring town of Skikda, a proportion between 75% and 90% of the building stock is based on reinforced concrete structure.

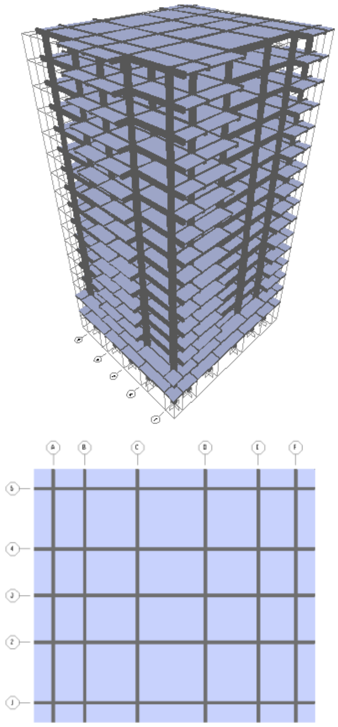

Fig. 2 The building structure (and a floor plan of the building)

In addition to that, the reinforced concrete frame structures were the most affected by damage after the last earthquakes.

This is due to the fact that the majority of construction build before the the beginning of 90th of the last century are designed according to an older version of the Algerian seismic regulations (RPA99 or RPA88). Moreover, some of these structures were built before the first Algerian Seismic Regulations (RPA 81) in 1981.

For this reason, the rehabilitation of reinforced concrete structures in Algeria, particularly in the north, becomes a necessity which is accompanied by a high work cost .

In order to illustrate the advantages of using the high performance concrete made from sand dune, an existing building located on the heights of the city of Skikda (situated in a high seismic zone) will be chosen.

The considered building is a reinforced concrete frame tower of 15 levels and a basement. Its rectangular shape has 27.20 m of length and 24.40 m of width. The total height of the tower is 51.25 m (Fig. 2). The structure is composed of columns (cross section dimensions varying between 0,25×0,25 and 0,7×0,7 m^2) and beams with a square section (cross section dimensions varying between 0,27×0,27 and 0,6×0,6 m^2) and ribbed floors of reinforced concrete having a thickness varying between 21 and 25 cm.

3. The Ultra high performance concrete

3.1 Aggregates

The aggregates used in this study come from two quarries in the north-east of Tunisia, the Jbel-Ressas for crushed aggregate (gravel 12/20, 4/12, 4/8 and crushed sand) and that of Khelidia for rolling sand. Rolling sand (RS) is a sand 0/2.5 mm low fine content, its chemical characteristics are shown in Table 1. The crushed sand is composed of particle with size ranging from 0.08 to 5 mm and with chemical characteristics (same as gravel) shown in Table 1.

For dune sand (DS), which comes from the Sahara desert in southern Tunisia, the chemical composition is presented in Table 1. The particle size of the sand is very fine and the maximum grain diameter is 0.4 mm. Granulometry curves of gravel are shown in Fig. 3, those of used sands are shown in Fig. 4.

The Sand Equivalent (SE) gives a global account of the amount of fine elements by expressing a conventional volumetric ratio between sandy elements which sediment and the fine elements which flocculate. This parameter measures the cleanliness of the sand. Table 2 shows that the sand equivalent of the three sands used is greater than 70. Therefore our sand is acceptable (NF P18-597).

3.2 Cement

The cement used is Portland cement CEM I 42.5, is produced by Jebel Jeloud factory. It has a compactness of 0.574 and a density of 3,210 g/cm^3. According to (Khouadjia *et al.* 2016), the cement Blaine specific surface is 346.6 m^2/kg and the mineralogical composition is that shown in the Table 3.

Table 1 Chemical composition of aggregates

Composition (%)	SiO_2	CaO	Al_2O_3	K_2O	Na_2O	MgO	Fe_2O_3	PF	SO_3
DS	93,7	1,8	0,2	0,36	0,38	0,26	1,58	1,31	-
CS	0,44	54,9	0,035	-	0,049	0,436	0,53	-	0,192
RS	98,2	0,08	0,34	0,17	-	-	0,11	-	-

Table 2 The Sand Equivalent

Sand	RS	CS	DS
Sand Equivalent	76	71	75

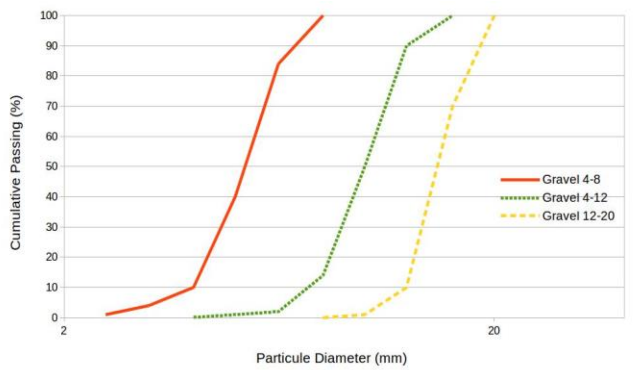

Fig. 3 Granulometry curves of gravel (Jbel Rsas)

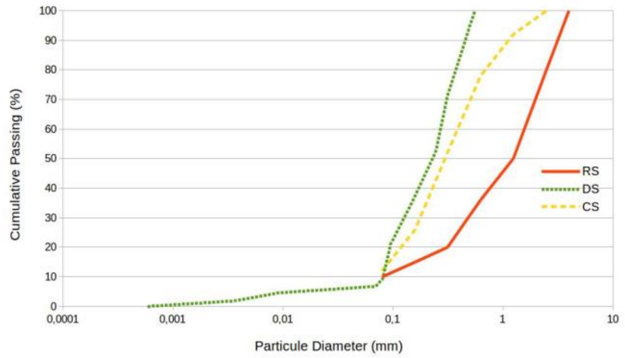

Fig. 4 Granulometry curves of sand

Table 3 Mineralogical composition of cement

C_3S	C_2S	C_3A	C_4AF
61%	11.85%	2.42%	13.75%

Table 4 Physico-chemical characteristics of Admixture

Density	pH	$(Na_2O)_{eq}$ (%)	Dry extract (%)	Cl^- (%)
1,060±0,020	5,5±1,0	≤1%	29,5%±1,4%	≤0,1%

Table 5 Formulations of concrete in kg

Designation	**G0**	**G01**	**G02**	**G1**	**G2**
Gravel 12/20	37,28	37,28	37,28	37,28	37,28
Gravel 4/12	30,7	30,7	30,7	30,7	30,7
Gravel 4/8	7,7	7,7	7,7	7,7	7,7
Rolling sand	20,01	20,01	20,01	19,41	19,41
Crushed Sand	13,35	13,35	13,35	13,08	13,08
Dune Sand				1,67	1,67
Cement	27	26,73	26,75	27	26,46
Slaked Lime		0,27	0,54		0,54
Admixture				0,54	0,54
Water	12,6	12,6	12,6	12,6	12,6

3.3 Admixture

The Admixture used is the Sika VISCOCRETE TEMPO 12 which is a super plasticizer based on polyacrylate copolymer. It has a reducing of water effect. Its physico-chemical characteristics are shown in Table 4.

3.4 Formulation of concrete

There exist many methods of formulating hydraulic mixtures. The basic principle of most of these methods is set in finding the maximum of the granular capacity. For this purpose, some methods use the measure of the compactness of the components and mixtures. Others use "a reference granular curve " assumed to give the maximum compactness with the used materials.

In North Africa (particularly in Algeria and Tunisia), to date, the most widely used method for formulating hydraulic mixtures is that of Dreux-Gorisse presented in

Dreux *et al.* (1998). In our work, the formulation of concrete is determined by this method, which was also applied in several research work such as Boumaza-Zeraoulia *et al.* (2013) and Yousfi *et al.* (2014). Further to the obtained results, five concrete formulations were retained, their composition is presented in Table 5.

The G0 formulation is a reference one. It contains neither admixture, nor slaked lime, nor sand dune. The G01 and G02 formations are used to observe the effect of slaked lime on the characteristics of concrete, whereas G1 and G2 will be used to show the sand dune effect. The total mass of sand in all formulations is the same.

3.5 Study of made concrete

3.5.1 Slump test

In accordance with the EN 12350-2 standard for the measurement of workability of concrete, recourse is given to the slump test with the Abrams cone. Table 6 shows the slump test results and the densities of the studied concretes. One notes that all the test values of workability vary between 10 and 13 cm, so we can say that the concrete used is very plastic (S3 consistency class). On the other hand, we see that the densities of concrete containing sand dune are superior to those of other types of concrete.

Table 6 Slump test and density of concrete

Designation		G0	G01	G02	G1	G2
Slump test (cm)		12,3	11	11	11	10,5
Density (g/cm^3)	Fresh	2,51	2,47	2,48	2,57	2,625
	Hard	2,468	2,45	2,437	2,54	2,58

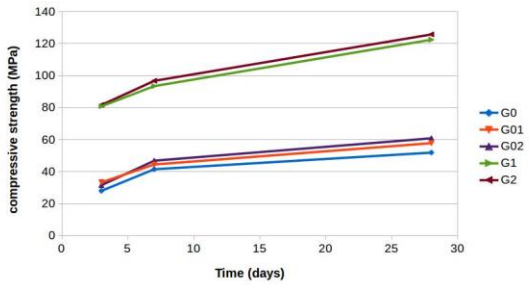

Fig. 5 Evolution of the compressive strength of concrete over time

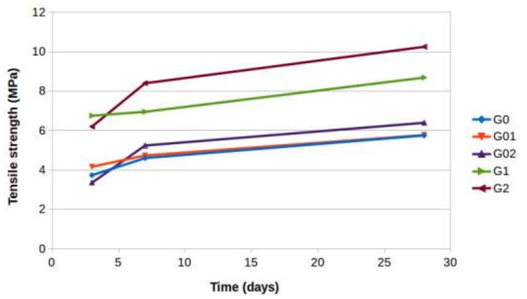

Fig. 6 Evolution of the tensile strength of the concrete over time

3.5.2 Compressive strength

To determine the capacity of the studied concrete, compression tests were performed on the different formulations of concrete while respecting standards NF P18411 and NF P18 412. Fig. 5 shows the variation of the compressive strength of concrete with time. In this figure, we can see that the dune sand concrete (G1) has a compression strength exceeding 80 MPa after 3 days and 122 MPa after 28 days, as opposed to 28 MPa after 3 days and 51 MPa after 28 days for the G0 formulation (reference concrete). This improvement is expected for the increase in density that induces an increase of compactness.

The evolution of the compressive strength of the ordinary concrete with added lime as a function of time shows that the addition of 1% lime gives the best results for three days while better results in the seventh and the 28th are days obtained with an addition of 2% lime. If the 28-day strength enhancement is 7.7% with 1% lime and 17% with 2% lime (in G01 and G02 compositions), it is only 2.4% between G1 and G2 manufactured with the sand dune.

3.5.3 Tensile strength

Tensile tests by flexural (3-point) were carried out while respecting the standard (P18-407). Fig. 6 shows a behaviour when using lime similar to that of the compressive strength: on the 3rd day, the greatest increase in strength obtained with 1% lime and the value is equal to 0.45%, but with 2% lime we have the best tensile strength on the 7th and 28th day. If the increase without sand dune is 11% at 28 days with 2% lime, this increase reaches almost 18% with the use of sand dune with a value of 10.25 Mpa.

3.5.4 Shrinkage study

The tests began with the G0 formulation (that does not contain lime). Then we studied the effect of the addition of 1% and 2% lime. This allowed to deduce, as shown in Fig. 7, that the addition 1% of slaked lime reduces the shrinkage with respect to the reference concrete, and that the addition of 2% leads to better results. Tests were carried out again on the high performance concretes made with dune sand previously used and studied. It is obvious that the addition of lime to the concrete minimizes the shrinkage. As expected, and because concretes based on dune sand are more compact, their shrinkage is lower than those of the reference formulations by 40%.

3.5.5 Swelling study

The swelling phenomenon was studied on samples stored in water. The from swelling as a function of time for different concretes is shown in Fig. 8. It is clear that the more lime added to the reference concrete, the more swelling increases. On the other hand, we see that the lime also increased swelling of the concrete made with the dune sand but, as expected, with lower values than those of the formulations G0, G01 and G02.

4. Assumptions and modelling

4.1 Characteristics of concretes

The building to be analysed has an ordinary reinforced concrete structure with compressive strength at 28 days of 25 MPa. The ultra high performance concrete used for reinforcing walls is that of the formulation G2. This formulation allows to obtain a compressive strength at 28 days that exceed 120 MPa. Table 7 shows the mechanical properties of the used concrete.

4.2 Characteristics of the steel

Table 8 shows the characteristics of the steel used in reinforced concrete.

4.3 Earthquake assumptions

According to the Algerian seismic rules RPA99/2003, the building is located an area of moderate seismicity (zone II), and since the building is a collective housing with a height that exceeds 48 m, it is classified in 1B group which includes constructions of high importance.

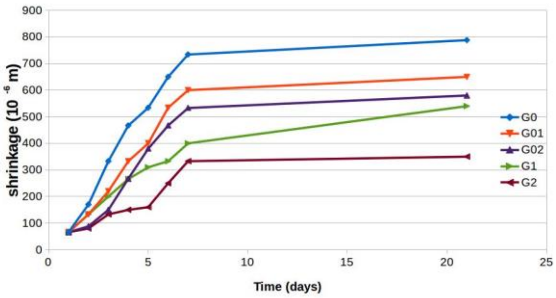

Fig. 7 Concrete shrinkage variation with and without the addition of the lime

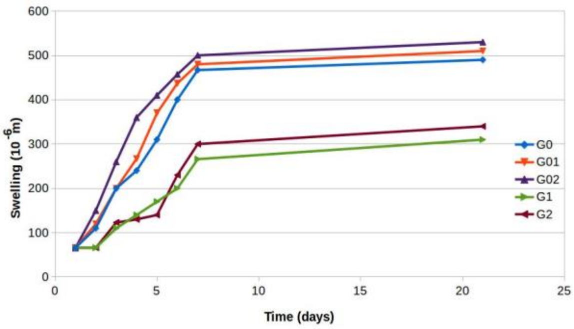

Fig. 8 Concrete swelling variation with and without the addition of lime

Table 7 Characteristics of concretes

Ordinary Concrete	Unit weight	25 kN/m^3
	Poisson's ratio	0,2
	Modulus of elasticity (MPa)	32164
	Compressive strength (28 days) (MPa)	25
UHPC	Unit weight	25 kN/m^3
	Poisson's ratio	0,2
	Modulus of elasticity (MPa)	54256
	Compressive strength (28 days) (MPa)	120

Table 8 Steel properties

Unit weight	78 kN/m^3
Modulus of elasticity	200000 MPa
Poisson's ratio	0,3
Yield strength	450 MPa
Ultimate strength	710 MPa
Ultimate strain	11%

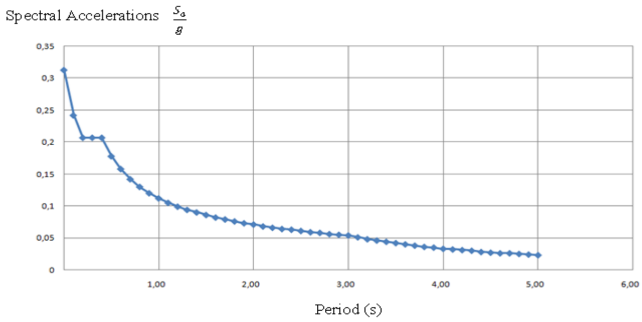

Fig. 9 Project Response Spectrum

According to the same regulations the site with its soft and highly altered rocks, is classified in the S2 category. Thus, the response spectrum considered in the project is that of Fig. 9.

4.4 Modelling assumptions

As indicated in Ismail (2014), when the objective is to calculate the non-linear capacity of an existing structure subject to horizontal loading with a reduced computational effort, pushover analysis in SAP2000 can obtain good accuracy.

Therefore, in this study, nonlinear finite element analysis is conducted using the "pushover" method in SAP2000 software. The same model and assumptions as in Trabelsi *et al.* (2011) are taken. A 3D model is used who columns and beams are modelled by Hermit finite element with six degrees of freedom and slabs are modelled by "shells" elements with dimensions of mesh 1 m×1 m. The connections between beams and columns are complete and the columns of the first level are considered embedded at the base.

The adopted model of the nonlinear behaviour of the reinforced concrete is an elasto-plastic model with work hardening. It have been derived from the standard FEMA356 2000 as shown in Fig. 10. The latter shows a typical response at a plastic hinge with an initial linear elastic behaviour followed by a perfectly plastic range and a final drop to a given residual strength.

In Fig. 10, point A represents the origin and B is the point of yielding; while point C correspond to the maximum force. The Plastic flow between B and C represents 10% of the total deformation of the steel and the values corresponding to points C, D, E have been derived from Table 6.18 of FEMA356 2000.

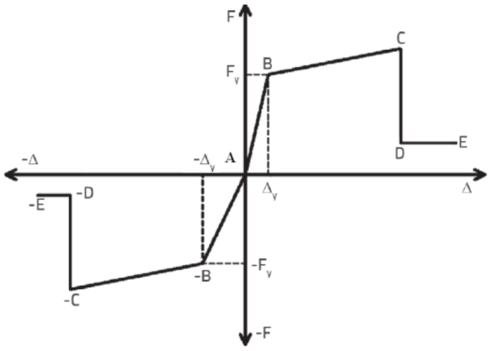

Fig. 10 Idealized force-deformation relationship (Erdem 2016)

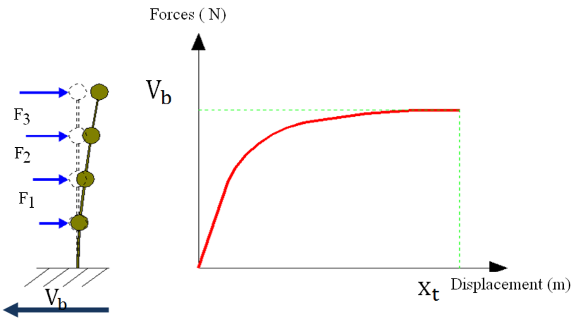

Fig. 11 Static analysis of structures (Petrini *et al.* 2004)

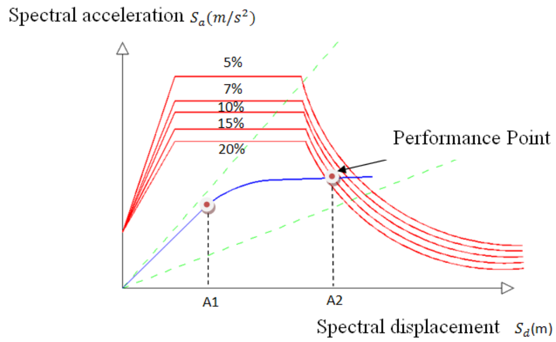

Fig. 12 Determination of the performance point (Trabelsi *et al.* 2011)

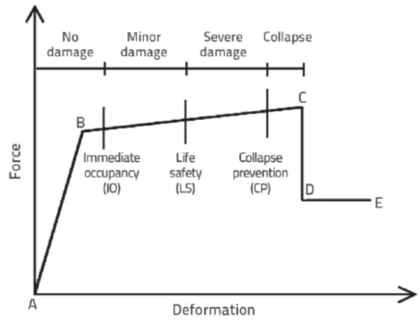

Fig. 13 Force-Deformation for Pushover Hinge (Erdem *et al.* 2016)

5. Analysis of the tower without reinforcement

5.1 Principle of the "pushover" method

The Pushover analysis developed over the past 20 years is a nonlinear static analysis for structure subjected to lateral loading. By considering a series of incremental static analysis, the pushover analysis evaluate the nonlinear behaviour of structures, and thus predicts the seismic force and the deformation demands. With that in mind, pushover analyses was carried out by applying a monotonically increased uniform distribution of lateral forces along the height of the structure until the limit of the acceptable plastique damage was reached. This allowed to establish the global capacity obtained by plotting the roof displacement versus base shear curve (Fig. 11).

The curve of Fig. 11 can be transformed into a capacity diagram by modifying the seismic force (base shear V_b) by a spectral acceleration S_a, and the roof displacement U_t by a spectral displacement S_d.

To determine the damage state of the structure, we proceed to the evaluation of the performance point. It is defined as the intersection of the capacity diagram of the structure with the inelastic spectrum under the seismic action to estimate the maximum displacement of the structure (Fig. 12).

Fig. 13 shows a general diagram of the damage state of a structure, and shows that the non-linear behaviour is composed of four segments.

As explained in Trabelsi *et al.* (2011), each segment corresponds to one of the damage states:

• The first level, Immediate Occupancy (IO part in Fig. 13), corresponds to the elastic behaviour of the structure. It represents a point where the seismic design level and the damage of the structure are superficial.

• The second level of damage (Life Safety LS) is a controlled level of damage. The stability of the structure is not questioned.

• The third level (Collapse Prevention CP), represents an advanced state of damage where the stability is in danger. Beyond this level, the structure is likely to collapse and will have no resistance.

5.2 Seismic analysis of the existing structures

For modelling a medium intensity earthquake, it is considered a seismic excitation with an estimated acceleration equal to 0.28 g.

Fig. 14 shows the resulting acceleration-displacement spectrum and the capacity curves of the structure in the horizontal direction (*x-x*).

Demand is high for the existing building since the performance point occurs between LS and CP event points, as shown in Fig. 14. The state of damage is advanced and the overall stability of the building is in danger. Therefore, retrofitting is imperative for the building.

6. R.C. shear walls retrofitting

View the unsatisfactory seismic behaviour revealed by the evaluation of the existing structure, RC shear walls are envisioned to reinforce the building.

Fig. 14 Performance point of the existing structure

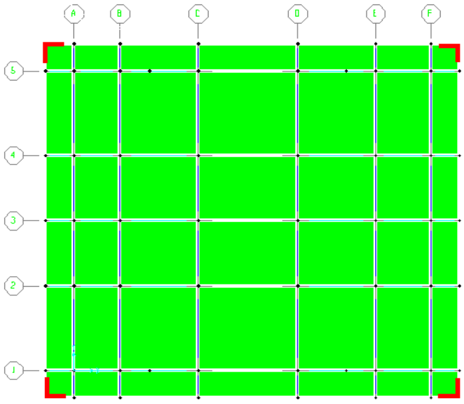

Fig. 15 Position of the R.C. shear wall in the structure

To facilitate implementation, the shear walls are executed at the corners of the building as shown in Fig. 15. Shear walls have a height of 59 m and a thickness of 25 cm. The width *L* which is common for all corners is considered variable.

Two alternatives of shear walls are considered. The first with an ordinary concrete and the second with the UHPC sand dune based.

6.1 Optimization of the width of reinforced concrete walls

To optimize the length *L* of the shear walls, several values of *L* are considered. The capacity curves of the strengthened building, presented in Fig. 16, show that when we use the UHPC the overall stiffness of the building and its resistance are increased.

Figs. 17 and 18 show the performance point associated to *L*=1 and 4 m for the two cases of concrete.

At every deformation step of the pushover analysis, the SAP 2000 program can determine the position and the FEMA limit state (IO, LS and CP) of the plastic rotation hinges in the structure. Fig. 19 shows the formation of plastic hinges in the direction (*x*-*x*) for some lengths of shear wall at the performance point.

It is observed that for *L*=1 m, the 4th floor is the weakest storey with plastic hinges formed at the top and bottom of some columns having reached the collapse state. For *L*=4 m, these columns reached the IO limit state.

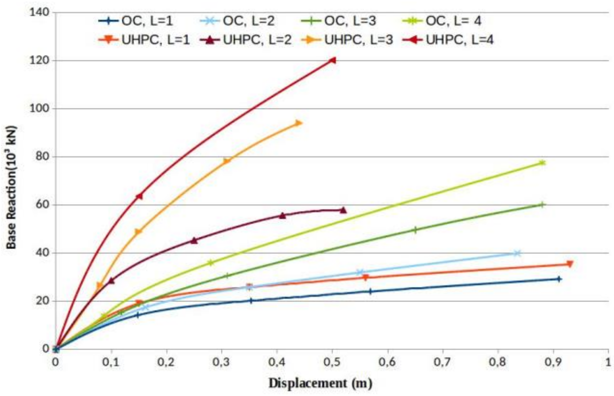

Fig. 16 Capacity curves of the structures retrofitted by different length of the R.C. shear walls

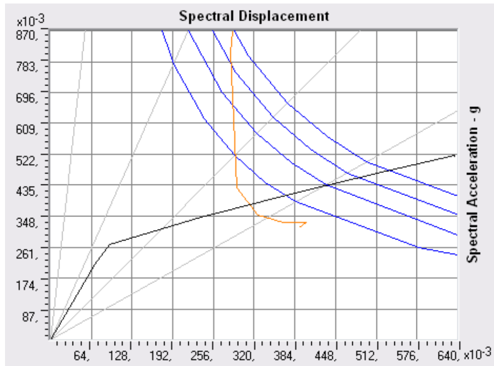

(a) *L*=1 m

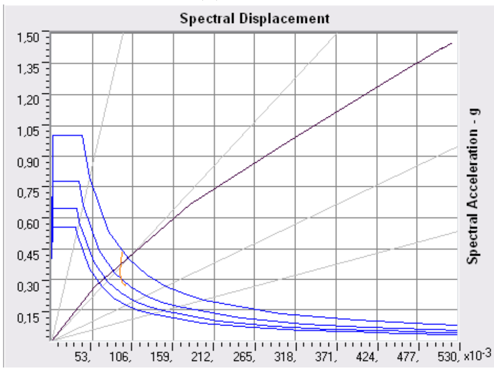

(b) *L*=4 m

Fig. 17 Performance point for the retrofitted structure using ordinary concrete

Based on the calculated performance points and the associated formation of plastic hinges, we illustrate the evolution of the behaviour of the retrofitted building depending on the shear wall length in figure 20.

It is shows that the damage state of the structure depends on parameter *L*. It is noted that to each state of damage in both concrete formulations, is associated a segment with different slope in the spectral displacement-acceleration space. Thus, for the same damage state “IO”, 3 m of width of ordinary concrete shear wall is equivalent to 1.5 m width of UHPC shear wall.

If we compare the two points of performance, reinforced structure with 1.5 m UHPC shear wall is slightly more rigid then that reinforced with 3 m of O.C shear wall.

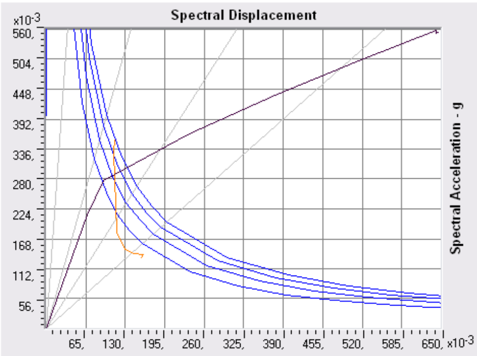

(a) L=1 m

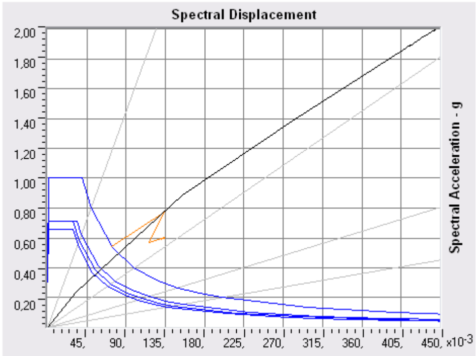

(b) L=4 m

Fig. 18 Performance point for the retrofitted structure using UHPC

Table 9 Weightage factors for Performance Range

Serial Number	1	2	3	4	5	6
Performance range	<B	B-IO	IO-LS	LS-CP	CP-C	C-D,D-E,>E
Weightage Factor (x_i)	0	0.125	0.375	0.625	0.875	1.00

6.2 Vulnerability analysis

A mesurement, that can be obtained from the pushover analysis, is the vulnerability index (Lakshmanan 2006). The vulnerability index is a measurement of the damage in a building defined as a weighted average of performance measures of the hinges in the components at the performance point.

The expression of the vulnerability index of a building is given as follows

$$VI_{bldg} = \frac{1.5\sum_i N_i^C x_i + \sum_j N_j^b x_j}{\sum_i N_i^C + \sum_j N_j^b} \qquad (1)$$

Where, N_i^c and N_j^b are the numbers of hinges in columns and beams, respectively, for the i^{th} and j^{th} performance range. x_i and x_j are the weightage factor assigned, respectively, for columns and beams. Table 9 shows the weightage factor for each performance range.

The performance ranges of the formed hinges are noted from the deformed shape output. The number of hinges formed in the beams and columns for each performance range are presented in Table 10.

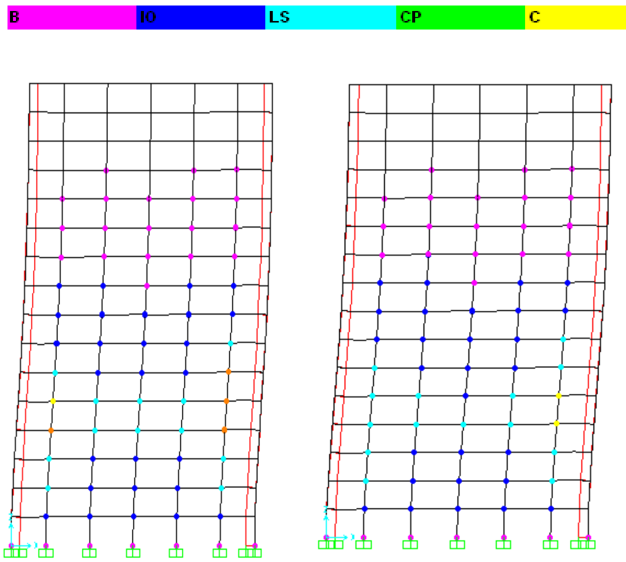

(a) L=1 m for O.C. (b) L=1 m for UHPC

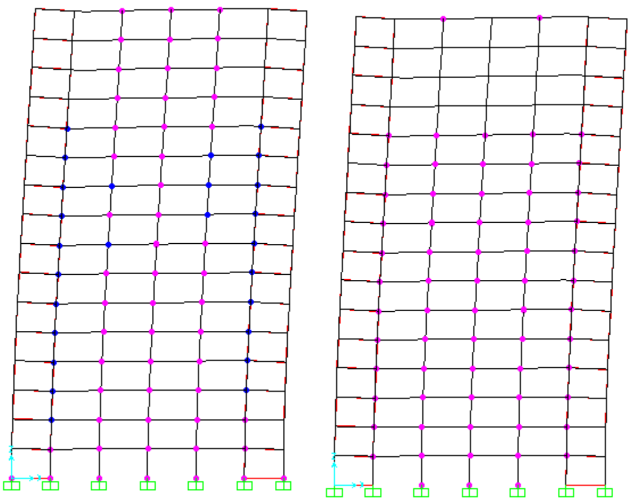

(c) L=4 m for O.C. (d) L=4 m for UHPC

Fig. 19 Comparison of hinging patterns at ultimate point for L=1 and 4 m

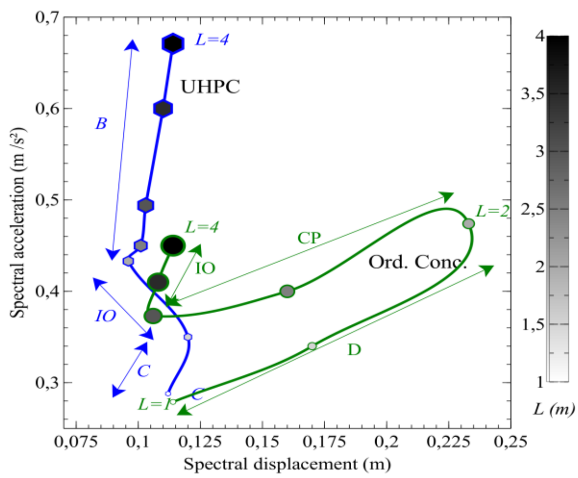

Fig. 20 Building performance points function of L

Table 10 Building hinge count and vulnerability index

Designation	Columns					Beams					VI_{bldg}
	Total	B-IO	IO-LS	LS-CP	D-E	Total	B-IO	IO-LS	LS-CP	D-E	
Existent building	1120	0	12	28	42	1050	0	11	7	37	0.0195
O.C. Retrofit (*L*=3 m)	1120	88	10	0	0	1050	76	3	0	0	0.0080
UHPC Retrofit (*L*=1.5 m)	1120	93	7	0	0	1050	89	8	0	0	0.0088

Table 11 Carbon fiber properties of carbon fiber

Unit weight of carbon fiber	17 kN/m^3
Young's modulus of carbon fiber	450000 Mpa
Poisson's ratio of the carbon fiber	0,2
Ultimate tensile strength	2500Mpa

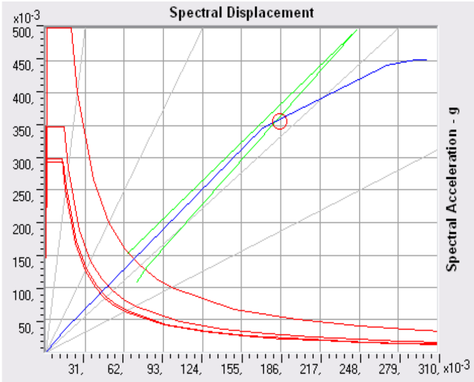

Fig. 21 Performance point for the retrofitted structure using carbon fiber sheets

Also, Table 10 gives the vulnerability index of the building. The obtained high value of VI_{bldg} for the existent building, compared to the retrofitted structure, reflects the poor performance and the high risk of the building. Besides, it can be seen see that the vulnerability index of the two reinforcement variants are very close.

7. Comparison with other retrofitting techniques

Two other different retrofitting techniques have been considered in this study to compare the results of the retrofitted building with RC shear wall: retrofitting with thin sheets of carbon fibers and retrofitting by the use of base isolators.

7.1 Retrofitting with carbon fiber sheets

Carbon fibers are very fine fibers with a diameter of 7 µm. They have excellent properties as the high strength, high elastic modulus, light weight, and high durability.

A carbon fiber sheet consists of carbon fiber strands arranged in the same direction. A carbon fiber strand consists of 12000 filaments of carbon fiber.

The reinforcement with carbon fiber sheets has the same behaviour as strengthening with additional external reinforcement. Indeed, it delays the concrete cracking and the plasticization of the reinforcement. Thus, the carbon fiber plates can improve the strength of the building against shear forces and bending moments (Priestley *et al.* 1996, Saadatmanesh *et al.* 1996, Saadatmanesh *et al.* 1997, Seible *et al.* 1997).

The sheet of carbon fibers (9mm thick), considered in the retrofitting of the building, are derived from a manufacturing by graphitization (Hamelin *et al.* (2001)), and their mechanical properties are shown in Table 11. The behavioural model of the sheet of carbon fibers is a brittle elastic model. In our case of study, the carbon fiber sheets are considered wound onto the surface of all the columns of the tower.

After simulation, the intersection between the demand curves and capacity occurs near the point IO event as shown in Fig. 21. The state of damage is superficial and the behaviour of the structure is improved.

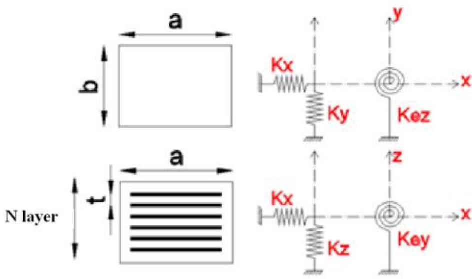

Fig. 22 Description of the Link/Support element (Rubbert insulator)

7.2 Retrofitting by base isolation

Base isolation is a technique that is generally used in rehabilitation of critical or essential structures. Its use permit to reduce the seismic impact on the building by increasing the natural period of the structure to increase displacements across the isolation level and reduced accelerations and displacements in the superstructure during an earthquake. For the building of our study, we consider that the isolation devices are inserted at the bottom of all columns.

The isolators are modeled in SAP2000 using Link/Support element (Rubber insulator) whose description is given in Fig. 22. It is assumed that the vertical stiffness is infinitely rigid (Kz=∞), the rotational stiffness are infinitely flexible ($K_{\theta z}=K_{\theta y}=K_{\theta x}=0$) and the horizontal stiffnesses are equal ($Kx=Ky$=2749 KN).

Fig. 23 shows the acceleration-displacement spectrum and the capacity curves of the structure in the horizontal direction (*x-x*). The intersection of the two curves takes place near the point event B; the response of the building remains perfectly elastic.

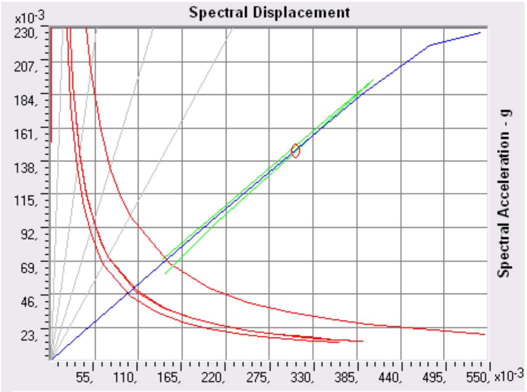

Fig. 23 Performance point for the retrofitted structure using base isolation

7.3 Economic study

The cost of retrofitting the analysed building by reinforced concrete walls, with all the direct and indirect costs, was estimated at around 137,810 Euros for ordinary concrete; and 75,030 for UHPC. The cost of building reinforcement with carbon fiber sheets was estimated at 261,956 Euros. The cost of building retrofitted by base isolation was estimated at 113,140 Euros.

Thus, in addition to meeting the technical criteria required by seismic standards, retrofitting the building through UHPC shear walls has significant technical and economic advantages. In fact, technically, the use of peripheral shear walls associated to the reduced length of 1.5 m on each side of the corners of the building allows limiting the intervention. Economically UHPC shear walls represents the least expensive solution with less than 29% of the cost of reinforcement by composite materials, and less than 55% of the cost of a reinforcement by ordinary concrete shear walls.

8. Conclusions

In Algeria, considering the importance of the damage caused by the earthquakes, a seismic retrofitting of existent buildings and especially those whose structure is made of reinforced concrete is necessary.

In order to reduce interventions in buildings, a new formulation of an ultra high performance concrete based on dune sand has was formulated in this paper.

Aggregates, sand equivalents, admixtures used and slump test, compression and tensile strength tests, shrinkage and swelling tests and final characteristics of the concrete are presented.

By determinning the characteristics of the concrete though testing, it is shown that the formulation of the UHPC made with dune sand allows to obtain a compressive strength at 28 days that exceed 120 MPa.

An existent reinforced concrete frame tower of 15 levels from Skikda city, that represents an unsatisfactory seismic behaviour, is considered.

Retrofitting by two variants of reinforced concrete shear walls were compared: ordinary concrete and UHPC made with dune sand.

A nonlinear dynamic analysis, based on the "Pushover" method has been conducted and results obtained in terms of demand, capacity and plastic hinges are given.

The analysis allowed an optimization of the width of reinforced concrete walls used in seismic strengthening for the two variants.

Thus, the study shows that, for the same damage state "IO", 3 m of width of ordinary concrete shear wall is equivalent to 1.5 m width of UHPC shear wall. Retrofitting with the retained width of the shear walls, is compared to the retrofitting with sheet of carbon fibers and the retrofitting by base isolation. The study shows great technical and economical advantages for UHPC shear wall retrofitting, these include a less cumbersome procedure, and a lower cost which is almost half of other retrofitting alternatives.

References

Algériennes RP. RPA 99/Version 2003. Ministère de l'habitat et de l'urbanisme. Centre national de recherche apliquée en génie-parasismique. Document technique reglementaire DTR-BC.;2.

Al-Harthy, A.S., Halim, M.A., Taha, R. and Al-Jabri, K.S. (2007), "The properties of concrete made with fine dune sand", *Constr. Build. Mater.*, **21**(8), 1803-1808.

Bouziani, T. (2013), "Assessment of fresh properties and compressive strength of self-compacting concrete made with different sand types by mixture design modelling approach", *Constr. Build. Mater.*, **49**, 308-314.

Boukri, M., Farsi, M.N., Mebarki, A., Belazougui, M., Amellal, O., Mezazigh, B. and Guessoum, N. (2014), "Earthquake loss estimation of existing buildings: Case of constantine city (Algeria)", *Second Conference on Earthquake Engineering and Seismology 2014*, Istanbul, Turkey, 25-29 August.

Boumaza-Zeraoulia, F. and Behim, M. (2013), "Formulation des bétons autoplaçants: Optimisation du squelette granulaire par la méthode graphique de Dreux-Gorisse", *Synthèse: Revue des Sciences et de la Technologie*, **27**(1), 63-72.

Cherifi, F., Farsi, M.N., Kaci, S., Belaidi, O. and Taouche-Kheloui, F. (2015), "Seismic vulnerability of reinforced concrete structures in Tizi-Ouzou City (Algeria)", *Procedia Eng.*, **114**, 838-845.

Chopra, A.K. and Goel, R.K. (2002), "A modal pushover analysis procedure for estimating seismic demands for buildings", *Earthq. Eng. Struct. D.*, **31**(3), 561-582.

Dreux, G. and Festa, J. (1998), *Nouveau guide du béton et de ses constituants*, Eyrolles.

D'aloia, L., Légeron, F., Le Roy, R., Runfola, P. and Toutlemonde, F. (2003), "Valorisation des betons a hautes performances dans les piles et pylones de grande hauteur des ouvrages d'art", Techniques et Methodes des Laboratories des Ponts et Chaussees-Guide Technique, (BETPIL).

Erdem, R.T. (2016), "Performance evaluation of reinforced concrete buildings with softer ground floors", *Građevinar*, **68**(01), 39-49.

Fajfar, P. (1999), "Capacity spectrum method based on inelastic demand spectra", *Earthq. Eng. Struct. D.*, **28**(9), 979-994.

FEMA-356: (Prestandard and Commentary for the Seismic Rehabilitation of Buildings), November, 2000, Washington, DC, Federal Emergency Management Agency.

Hamelin, P. and Ferrier, E. (2001), "Etude bibliographique sur les renforcements par matériaux composites de structure du génie civil-Comportement en fatigue et en fluage des renforcements, Identification des problèmes liés aux renforcements par composites", *Cahier des charges essai de fatigue, Rapport NLCPC/01 du*, **27**(04), 01.

Ismail, A. (2014), "Non linear static analysis of a retrofitted reinforced concrete building", *HBRC J.*, **10**(1), 100-107.

Jiménez, M.J. and Garcia-Fernandez, M. (1999), "Seismic hazard assessment in the Ibero-Maghreb region", *Ann. Geophys.*, **42**(6), 1057-1065.

Khouadjia, M., Mezghiche, B. and Drissi, M. (2016), "Évaluation expérimentale et numérique de la résistance à la compression des bétons à base des sables de carrière modifiés avec sable de dune", Courrier du Savoir, 20.

Konkov, V. (2013), "Principle approaches to high performance concrete application in construction", *Procedia Eng.*, **57**(1), 589-596.

Lakshmanan, N. (2006), "Seismic evaluation and retrofitting of buildings and structures", *ISET J. Earthq. Technol.*, **43**(1), 31-48.

Luo, F.J., He, L., Pan, Z., Duan, W.H., Zhao, X.L. and Collins, F. (2013), "Effect of very fine particles on workability and strength of concrete made with dune sand", *Constr. Build. Mater.*, **47**, 131-137.

Mazza, F. (2015), "Comparative study of the seismic response of RC framed buildings retrofitted using modern techniques", *Earthq. Struct.*, **9**(1), 29-48.

Ousalem, H. and Bechtoula, H. (2005), "Inventory survey of the 2003 Zemmouri (Algeria) earthquake: Case study of Dergana City", *J. Adv. Concrete Technol.*, **3**(1), 175-183.

Petrini, L., Pinho, R. and Calvi, G.M. (2004), *Criteri di progettazione antisismica degli edifici*, Iuss Press

Priestley, M.N., Seible, F. and Calvi, G.M. (1996), *Seismic design and retrofit of bridges*, John Wiley & Sons.

Rmili, A., Ben Ouezdou, M., Added, M. and Ghorbel, E. (2009), "Incorporation of crushed sands and tunisian desert sands in the composition of self compacting concretes Part I: Study of formulation", *Int. J. Concrete Struct. Mater.*, **3**(1), 3-9.

Saadatmanesh, H., Ehsani, M.R. and Jin, L. (1996), "Seismic strengthening of circular bridge pier models with fiber composites", *ACI Struct. J.*, **93**(6), 639-738.

Saadatmanesh, H., Ehsani, M.R. and Jin, L. (1997), "Repair of earthquake-damaged RC columns with FRP wraps", *ACI Struct. J.*, **94**, 206-215.

Seible, F., Priestley, M.N., Hegemier, G.A. and Innamorato, D. (1997), "Seismic retrofit of RC columns with continuous carbon fiber jackets", *J. Compos. Constr.*, **1**(2), 52-62.

Trabelsi, A., Mekki, O.B. and Hassis, H. (2011), "Analyse sismique non linéaire d'un bâtiment classé renforcé par des plaques minces en fibres de carbone", *Eur. J. Environ. Civ. Eng.*, **15**(3), 367-389.

Yousfi, S., Nouri, L., Saidani, M. and Hadjab, H. (2014), "The use of the dreux-gorisse method in the preparation of concrete mixes: an automatic approach", *Asian J. Civ. Eng. (BHRC)*, **15**(1), 79-93.

Zeghichi, L., Benghazi, Z. and Baali, L. (2012), "Comparative study of self-compacting concrete with manufactured and dune sand", *J. Civ. Eng. Architec.*, **6**(10), 1429.

AG